Journal of Saudi Chemical Society (2015) **19**, 537–548

King Saud University

Journal of Saudi Chemical Society

www.ksu.edu.sa
www.sciencedirect.com

ORIGINAL ARTICLE

Spent wash decolourization using nano-Al_2O_3/kaolin photocatalyst: Taguchi and ANN approach

Charles David [a], **M. Arivazhagan** [a,*], **Mohamed Ibrahim** [b]

[a] *Environmental Biotechnology Research Laboratory, Department of Chemical Engineering, National Institute of Technology, Tiruchirappalli 620 015, Tamil Nadu, India*
[b] *Department of Mechanical Engineering, National Institute of Technology, Tiruchirappalli 620 015, Tamil Nadu, India*

Received 27 February 2015; revised 22 May 2015; accepted 30 May 2015
Available online 6 June 2015

KEYWORDS

Spent wash decolourization;
Al_2O_3 nanoparticle;
Kaolin;
Photocatalysis;
Taguchi;
ANN

Abstract The intense colour of the spent wash effluent leads to crucial ecological issue when released untreated into the environment. The decolourization of distillery spent wash effluent is known to be a very challenging task. In this study, the degradation of organic pollutants in the form of colour was performed using nano photocatalyst prepared using aluminium oxide (Al_2O_3) nanoparticle and kaolin clay. As-synthesized nano-Al_2O_3/kaolin composites were used as photocatalyst for colour degradation of spent wash effluent. The process parameters such as dosage, pH, temperature and agitation were optimized to attain the maximum decolourization efficiency. The structural and the textural characteristics of the photocatalyst were analysed by X-ray diffraction (XRD), Brunauer–Emmett–Teller (BET) surface area analysis, High Resolution Scanning Electron Microscope (HRSEM) and Energy Dispersive X-ray (EDAX). Optimization of the process parameters using Taguchi Orthogonal Array (OA) design resulted in a maximum of 80% spent wash decolourization. Using Artificial Neural Network (ANN), a two layered feedforward back-propagation model resulted as the best performance and predictive model for spent wash decolourization. The experimental data were found to be in excellent agreement with the predicted results from the ANN model.

1. Introduction

Molasses based distilleries are one among the major industries which expel huge quantities of high strength wastewater which has extreme potential towards causing tremendous water pollution. Spent wash is generally characterized with an unpleasant odour and highly recalcitrant dark brown colour [1]. The intense colour is due to the presence of a dark brown pigment known as melanoidin. Melanoidin is a group of polymeric

* Corresponding author. Tel.: +91 94874 12478.
E-mail address: ariva@nitt.edu (M. Arivazhagan).
Peer review under responsibility of King Saud University.

Production and hosting by Elsevier

http://dx.doi.org/10.1016/j.jscs.2015.05.012

compounds which are a product of the Maillard reaction, a non-enzymatic reaction between sugars and amino compounds [2,3]. The empirical formula of melanoidin is $C_{17–18}H_{26–27}O_{10}N$ [4]. This recalcitrant low or high molecular weight polymer is very tenuous to get degraded by the conventional biological treatment methods such as the anaerobic digestion, anaerobic lagoons and activated sludge process and is found ineffective [5,6]. When the untreated effluent gets released into surface water resources, the dark colouration of melanoidin hinders the penetration of sunlight into the water, thereby decreasing the photosynthetic activity and eventually affecting the life of aquatic microbiome [7]. Moreover, the high concentrations of chemical oxygen demand (COD), biochemical oxygen demand (BOD) and biodegradable organic materials, namely carbohydrate, lignin, hemicellulose, dextrins and organic acids [8,9] were also commonly present in the distillery spent wash effluent. Hence, disposing distillery effluent into the environment without proper treatment is hazardous to the ecosystem and has a high pollution potential [10]. Since the spent wash contains highly stable suspended colour pigments which cannot be separated with conventional physical treatment methods such as filtration or settling, there is always a lookout for advanced treatment methods.

Al_2O_3 nanoparticle has enormous industrial applications and has been widely used as catalysts, catalytic supports and as adsorbents [11,12]. Powdered Al_2O_3 was always preferred to bulk Al_2O_3. Kaolin is a soft, earthy, usually white mineral, formed by chemical weathering of aluminium silicate minerals such as feldspar. It is one of the most abundantly available minerals in soil sediments which is a common weathering product of many tropical and sub-tropical soils [13–15]. Kaolin is planar hydrous phyllosilicate clay, belonging to an interlayer structural class. Kaolinite possesses a dioctahedral structure having structural dimension in the nanometre range and the thickness is about 0.7 nm [16]. Even though kaolin has a low cation exchange capacity of 3–15 meq/100 g, it possesses adsorption properties that are strong enough to scavenge organic and inorganic pollutants present in the water [17]. Several works have been reported stating the usage of kaolin as an adsorbent for treating cationic dyes like malachite green [18], methylene blue [17], crystal violet and brilliant green [19]. Moreover, as a cheap and widespread industrial mineral, kaolin has been proven to be a good source of aluminium [20]. Kaolin also consists of non-phyllosilicate minerals such as carbonates, feldspars and quartz together with the (hydr) oxides of iron and aluminium, which are referred to as 'non-clay constituent' or 'accessory minerals' [14,16]. Kaolin has been a very useful and versatile domestic and industrial material known much before the industrial revolution and the oldest known use of the kaolin is as a ceramic raw material [21]. The other uses of kaolin include applications in medicine, coated paper, paint and construction [22]. Thus, using cheap and abundantly available kaolin to partly replace nano-Al_2O_3 is cost effective and practical approach.

The recent studies comprising nanocomposites of $Ag@TiO_2$, $AuTiO_2$, $AgCeO_2$ and $Au@CeO_2$, synthesized by biogenic and green approach using electrochemically active biofilms (EABs) showed exceptionally high photodecomposition efficiency towards degradation of methyl orange and methylene blue dyes under visible light irradiation which was highly efficient compared to pure TiO_2 and CeO_2. Moreover, these nanocomposites were also found to be exceptionally more stable and reusable [23–26]. Recent literatures found nanorods of pure ZnO, prepared by direct calcination of zinc acetate dihydrate to be photocatalytically active under UV light irradiation [27]. Nanorods of Hg doped ZnO, prepared by the facile thermal decomposition method were capable of degrading model organic dyes under visible light condition [28]. Nanorods of ZnO, ZnO/CuO and ZnO/CdO nanocomposites were synthesized by the thermal decomposition method. The photocatalytic activity of ZnO/CdO and ZnO/CuO nanocomposites was tested for the degradation of organic dyes such as methylene blue and methyl orange in aqueous medium under visible light irradiation. The photo catalytically active composite materials were able to degrade real textile waste water under visible light illumination [29,30].

Artificial Neural Networks (ANNs) have been a great interest over the last decade and are being successfully applied across a range of problem solving domains such as finance, medicine, engineering, geology and physics. This computational tool can be employed where there are problems of prediction, classification, modelling, simulation or control [31,32]. It is considered as a black-box device that receives input, transmits and produces output [33,34]. Basically, for a network to work, a set of input and output data are necessary. Compared to the design of experiments, ANN requires more number of training data which is a major drawback and it can be rectified using the statistical experimental design, data comprising the minimum number of experiments as input data for the ANN model. The network is trained with a set of experiments, consisting values of both input and output variables. Further, the network is tested with a series of experimental inputs to check whether the trained network is able to reproduce original experimental outputs [35,36].

The neural network is a highly adaptable system with the capacity to learn relationships through repeated feeding of data and is capable of predicting new data. The principle of ANN is to obtain a number of outputs (response variables) from a number of inputs (measured data), using a series of layers of artificial neurons which are interconnected between them [37]. The input and output data correspond to the sensory nerves and the motor nerves of a typical biological system. There are hidden neurons, which play an internal role in the network. The input, the hidden and the output neurons must be connected together. The algorithm progresses iteratively through a number of epochs. On each epoch, training cases are submitted to the network. The target and the actual outputs are compared to calculate the error. This error, together with the error surface gradient, is used to adjust the weights, and then the process repeats. The initial network configuration is random and the training stops when a given number of epochs elapse or when the error reaches an acceptable level or when the error stops improving [31].

The significance of this study is the novel initiative to combine the aluminium oxide nanoparticle with inexpensive kaolin clay and utilization of the as-synthesized as photocatalyst for the degradation of spent wash effluent in the presence of visible light irradiation. The objective of this study is to investigate the photocatalytic degradation of distillery spent wash in terms of colour removal in the presence of a visible light source and nano-Al_2O_3/kaolin as composite photocatalyst. The major process parameters were optimized using Taguchi Orthogonal Array (OA) design of experiment. The effect of the key operating parameters, *viz*. catalyst dosage, pH,

temperature and agitation speed in the presence of visible light irradiation for the decolourization of real spent wash was studied. Experimental data were validated and predicted using ANN tool to check the performance of the experiment.

2. Material and methods

2.1. Collection of distillery spent wash effluent

The raw spent wash effluent was collected in sterile sampling bottles from a local distillery industry near Tiruchirappalli, India and stored in the refrigerator at 4 °C. The concentrated effluent was diluted to 10% of its original concentration using distilled water and its physico-chemical characteristics are listed in Table 1.

2.2. Preparation and characterization of nano-Al_2O_3/kaolin photocatalyst

Aluminium oxide (Al_2O_3), NanoDur®, 99.5% pure, was procured from Alfa Aesar, UK. The particle size was in the range of 40–50 nm and surface area of 32–40 m^2/g. Kaolin ($Al_2Si_2O_5(OH)_4$), hydrated aluminium silicate, extra pure, was procured from HiMedia and used as received. The average surface area of the raw kaolin was 12–16 m^2/g with a particle size of 70–100 nm. Al_2O_3/kaolin composite nano photocatalyst was prepared by heating equal parts of aluminium oxide and kaolin at 800 °C for 6 h in a box furnace. The nano composite, hence formed was stored in a desiccator till further usage.

X-ray diffraction (XRD) patterns were recorded using a Rigaku, Ultima-IV, powder X-ray diffractometer with Cu kα radiation (λ = 1.54056 Å), 2θ range of 10–90° and scanning speed of 2°/min. Micrographs were obtained using a Hitachi Model S4800 High Resolution Scanning Electron Microscope (HRSEM). The samples were sputter coated with a thin layer of gold for uniform charge dissipation during high resolution SEM imaging. The ion sputter coater (Hitachi E1010) was operated using a current of 15 mA for 30 s. The Energy Dispersive X-ray (EDAX) analysis to evaluate the purity in terms of elemental compositions of the sample was performed using Horiba EDAX equipment mounted on the SEM instrument. The surface area of the samples was determined by Brunauer–Emmett–Teller (BET) method in which, samples were preheated in the presence of nitrogen using Belprep Vac II. The sample was loaded into the cell tube and weighed. The samples were degassed at 250 °C for two hours at a vacuum pressure of 10^{-2} kPa. The difference in the weight of the sample before and after degassing yielded the sample quantity. The surface area and the porosity of the adsorbents were analysed using volumetric gas adsorption methods (Belsorp Mini II). The sample cell containing degassed sample was loaded in the Belsorp Mini II instrument. Adsorption and desorption onto the sample occurred and the surface area was evaluated.

2.3. Experimental design for optimization of the decolourization process

A five-level-four-factor Taguchi Orthogonal Array (OA) design was employed using Minitab statistical software to generate experimental runs by considering four independent input variables *viz*. Catalyst dosage (*A*), pH (*B*), temperature (*C*) and agitation speed (*D*). The percentage colour removed was the output response. Based on the literature and preliminary experiments, the minimum and the maximum range levels of the process parameters were fixed. The range of controlling factors was in the range of 0.5–2.5 g/l for catalyst dosage, pH 3–11, temperature 25–45 °C and agitation speed 50–250 rpm. The treatment time with visible-light illumination was fixed for three hours. The experimental values and the range levels are tabulated in Table 2.

2.4. Photocatalytic decolourization of spent wash

The batch photocatalytic degradation was performed in Erlenmeyer flasks (250 ml volume) containing 100 ml of spent wash effluent. The appropriate dosage of the nano photocatalyst was added and the pH of the effluent was adjusted using dilute NaOH and HCl. The batch was sonicated for 10 min to attain the uniform suspension of the catalyst. The batch flasks were shifted to an incubator shaker and prior to visible-light illumination, the suspension was stirred mildly for 30 min under complete darkness in order to allow the nanoparticle to attain adsorption/desorption equilibrium. Then, the reaction solution was stirred under visible light irradiation sourced by two fluorescent lamps (24 W, Philips) equipped with a wavelength pass filter at 420 nm to block UV radiation. The lamp was placed 10 cm above the reaction flasks. The flasks were kept open to ensure adequate oxygen to get mixed in the reaction solution. After 3 hours, aliquots of samples were withdrawn and centrifuged at 10,000 rpm to remove the particles. The degradation in colour was measured at a characteristic wavelength of 475 nm using UV–Visible spectrophotometer (Spectroquant, Pharo 300, Merck).

The percentage colour removal was calculated by:

Table 1 Physico-chemical characteristics of distillery spent wash (10% diluted) [30].

Parameters	Values
pH	5.5–6.0
Temperature (°C)	30 ± 2
Colour	Dark brown
Odour	Burnt sugar
COD (mg/l)	14,000–16,500
Turbidity (NTU)	490–510
Absorbance at 475 nm	2.01

Table 2 Coding of experimental factors and levels of Taguchi design.

Factor	Symbol	Coded levels				
		−2	−1	0	+1	+2
Dosage (g/l)	*A*	0.5	1.0	1.5	2.0	2.5
pH	*B*	3	5	7	9	11
Temperature (°C)	*C*	25	30	35	40	45
Agitation speed (rpm)	*D*	50	100	150	200	250

$$\% \text{ colour removed} = \frac{C_0 - C_t}{C_0} \times 100 \quad (1)$$

where, C_0 and C_t are the initial absorbance and absorbance at time t for the spent wash at a corresponding wavelength of 475 nm [38–40].

2.5. Artificial Neural Network for predicting the decolourization efficiency

Experimental data on the photocatalytic degradation were trained and validated using the ANN tool in MATLAB. The four process parameters such as catalyst dosage, pH, temperature and agitation speed were considered as the input variables and the experimental response in terms of decolourization efficiency was considered as the output variable. Experimental data were fed into the ANN tool by considering some initial guess such as feedforward backpropagation, mean square error (MSE) method. The performance of the neural network depends on the number of hidden layers and the number of neurons per hidden layer. A few attempts were made to select the best architecture for the neural network by altering the number of hidden layers as well as the number of neurons in each hidden layer. For the iteration to be complete and to obtain the converged result, every time the loop had to be altered such that, the regression and the epoch reached the minimum value until its validation gets stopped. The initial time was set as normal so that the method took its own time to attain the minimum value. In our study, the structure of the neural network was 4–10–10–1 (4 neurons in the input layer, 10 neurons in the first hidden layer, 10 neurons in the second hidden layer and 1 neuron in the output layer) as shown in Fig. 1. The neurons are based on the PURELIN transfer function. The network was trained using the TRAINLM (Levenberg–Marquardt) algorithm and mean squared error (MSE) was used as the performance function which was to be minimized to 1×10^{-10}. All other ANN parameters were set as default values as in the ANN tool, MATLAB. The network was trained for 1000 iterations. The ANN summary of this study is shown in Fig. 2.

When the iteration reached the minimal gradient value, the performance validation and the regression were tested. It was observed from the performance plots (Fig. 3) that, the values of the fixed data, validation trial and the performance almost converge with the best fit line. It was also concluded that the experiments as well as the theoretical trials comparatively had the minimal error correspondingly, the gradient reaches minimum of $10^{1.1}$ at epoch 3.

From the regression analysis, the validation, trial target was dealt. From Fig. 4, it was noted that the fit data line and the cluster line almost coincided with each other with an R value of 0.99244, 0.95256 and 0.95273 for training, validation and test respectively. Since the R value approached almost 99%, it could be interpreted that the experimental error was minimized and the experimental data and model predictions were in excellent agreement.

3. Results and discussion

3.1. Nano-Al_2O_3/kaolin photocatalyst preparation and characterization

In this study, the possible use of aluminium oxide nanoparticle and kaolin clay composite as a nano photocatalyst for spent wash colour degradation was investigated. The nano-Al_2O_3/kaolin composite [Al_2O_3: kaolin (wt: wt) = 1: 1] was characterized in detail. The XRD patterns of the nano-Al_2O_3/kaolin are shown in comparison with the XRD patterns of pure forms of Al_2O_3 and kaolin in Fig. 5(a–c). From the

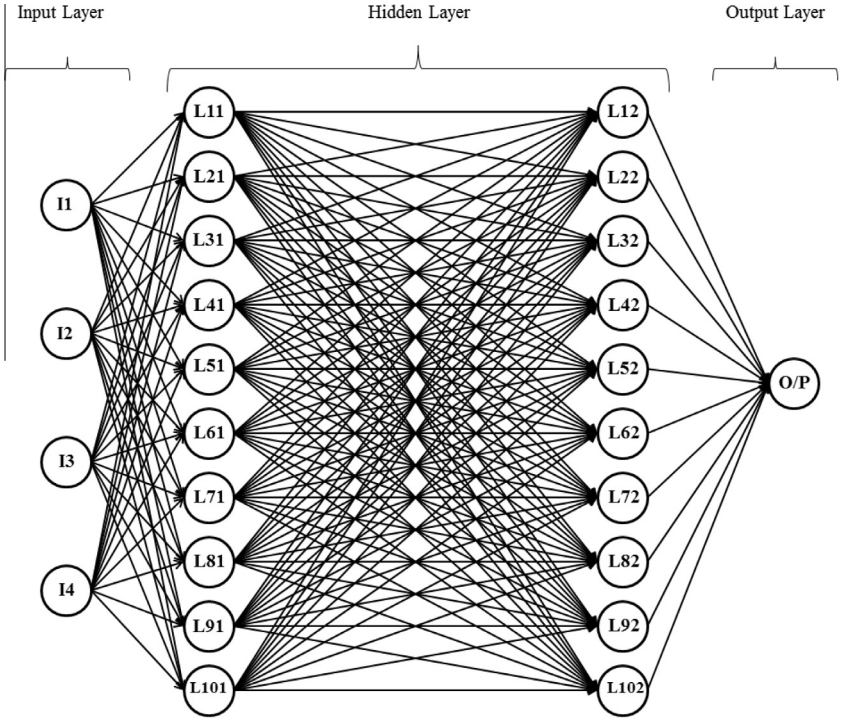

Figure 1 Architecture of Artificial Neural Network (ANN).

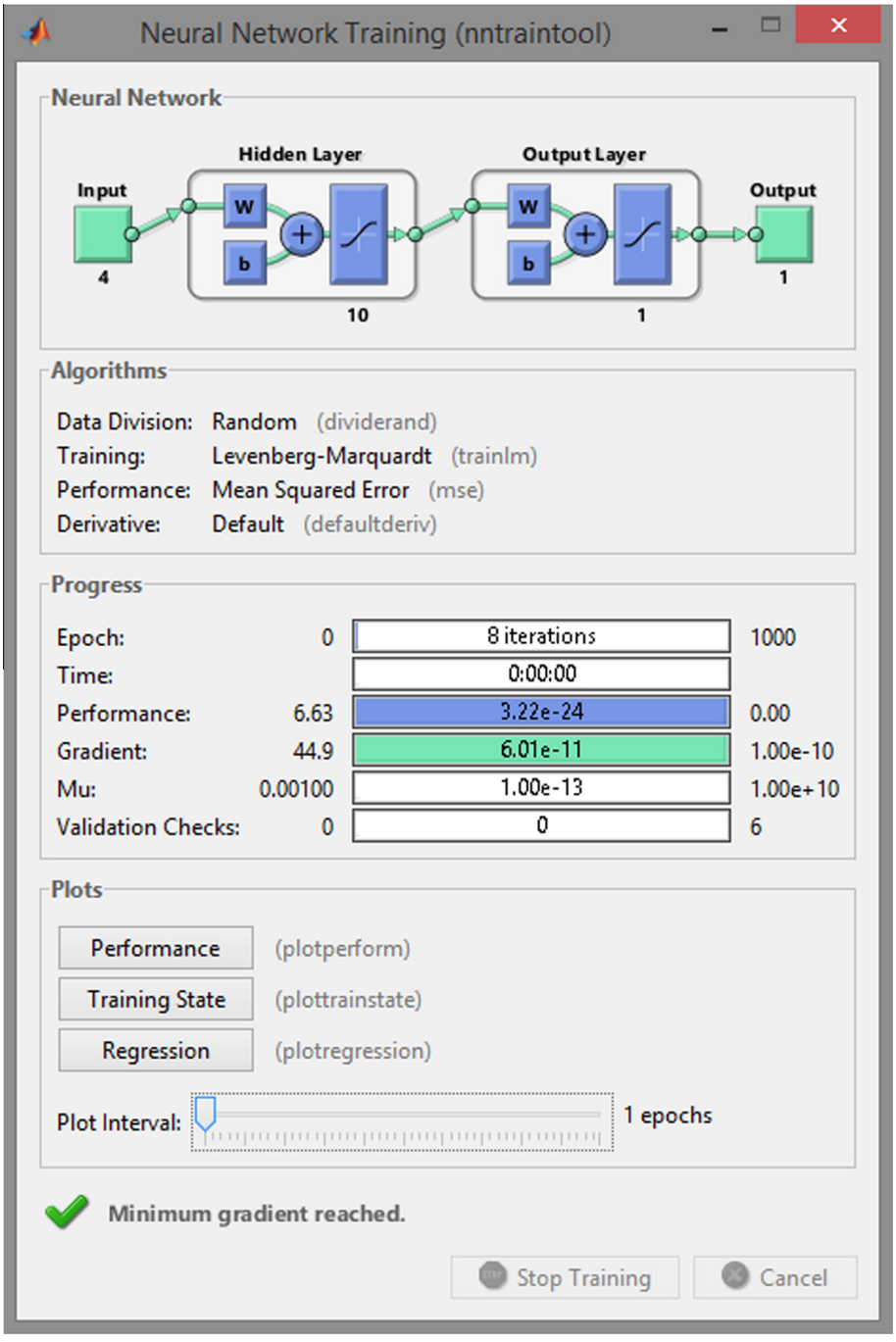

Figure 2 Summary of ANN modelling.

XRD profile of aluminium oxide nanopowder, two main diffraction peaks can be noticed denoting the crystalline nature of nano-Al_2O_3. From the XRD profile of kaolin, the signature peaks for aluminium silicate hydroxide with a high intensity of reflections can be seen, whereas, in the XRD profile of nano Al_2O_3/kaolin, the intensity peaks of aluminium oxide were observed remarkably lessened, which denotes that the calculation process at 800 °C has converted the composite into a milder amorphous form. Similarly, the complete absence of high intensity peaks of kaolin is due to the reason that, de-hydroxylation of kaolin above 550 °C converts crystalline kaolin into an amorphous form [41]. Although kaolin was not obviously destroyed during the synthesis process, there were changes in the XRD pattern of the composite compared with that of pure kaolin. The relative intensity of the XRD peaks shows kaolin was remarkably weakened in the composite. The X-ray diffraction was influenced due to the deposition of Al_2O_3 nanoparticle into the interlayer spaces present in the kaolin, which was also confirmed by the SEM images [42].

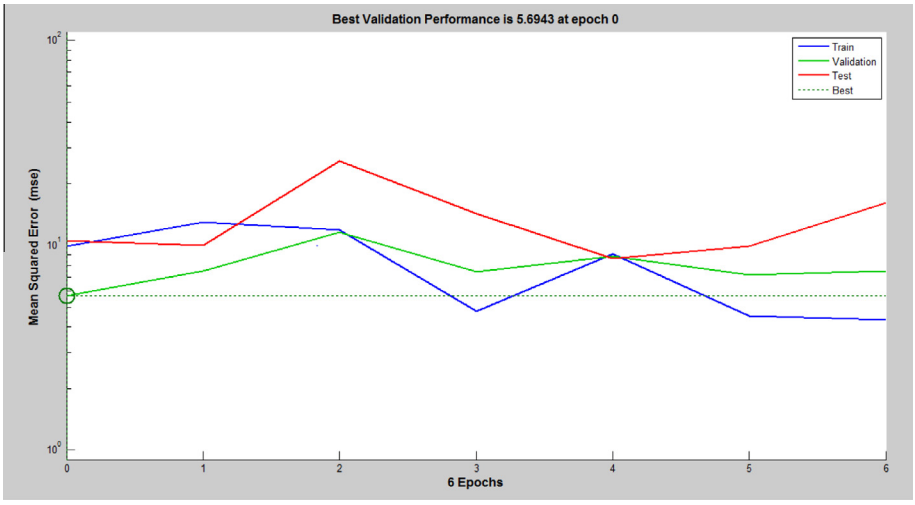

Figure 3 ANN performance plot.

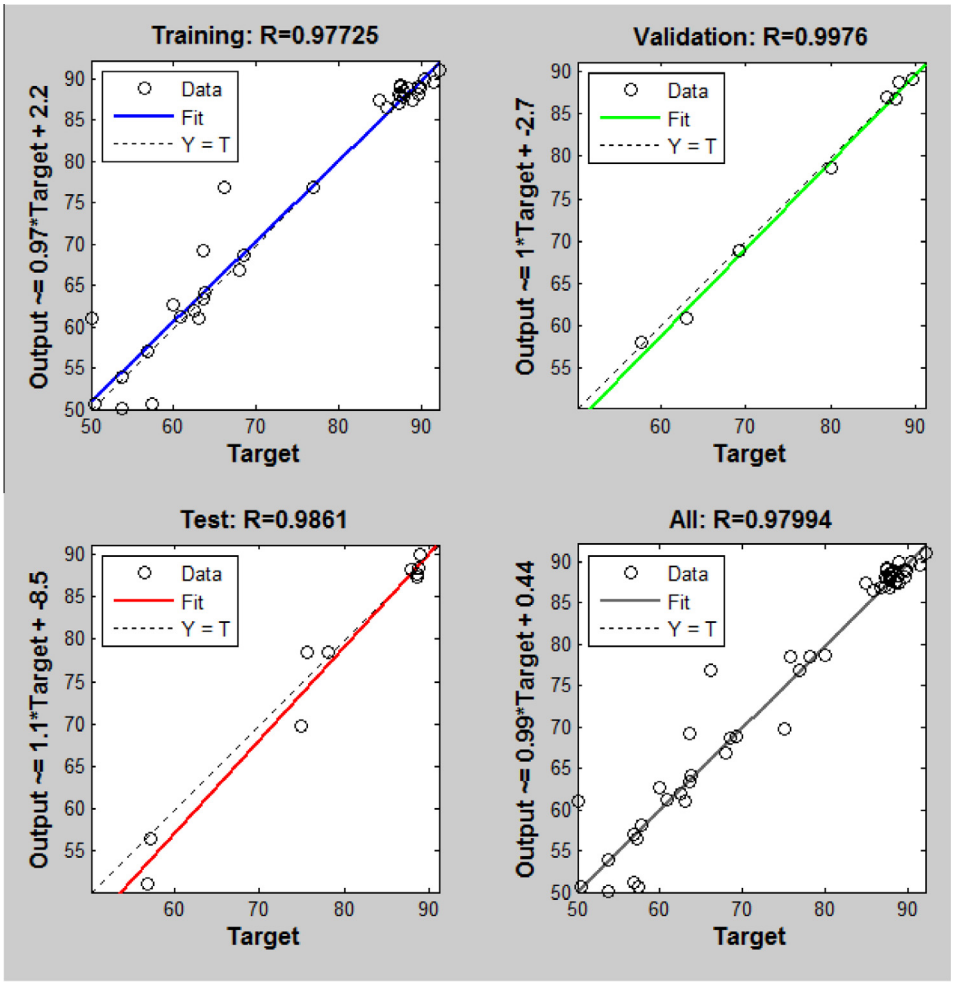

Figure 4 Parity plots of predicted values versus experimental values (training, testing and validation).

SEM images of Al_2O_3 nanoparticle, nano-Al_2O_3/kaolin composite and raw kaolin are shown in Fig. 6(a–c). From the SEM micrograph, it can be clearly visualized that the kaolin structure consisted of numerous smooth sheet like flakes which were stacked upon adjacent sheets forming a huge number of pores in which the nano-Al_2O_3 particles were found deposited. Many of the other Al_2O_3 nanoparticles were also seen scattered all over the surface of the kaolin structure.

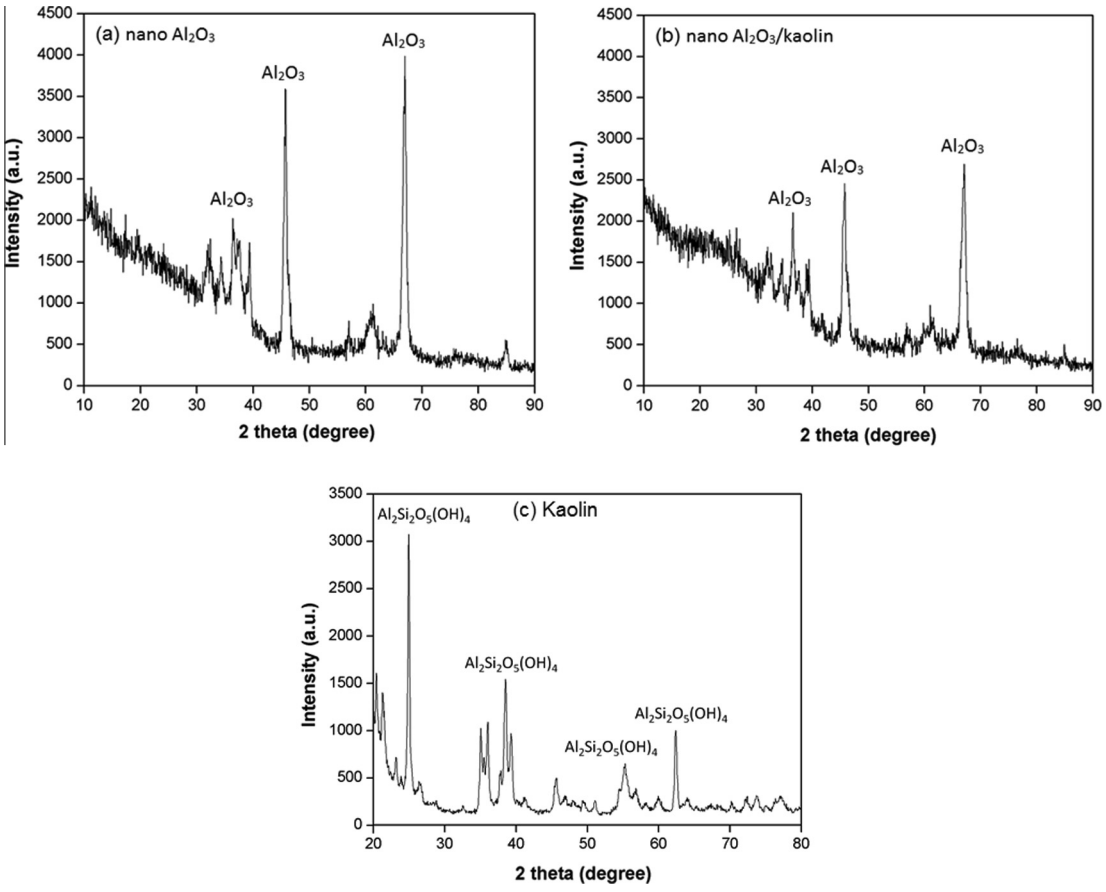

Figure 5 XRD diffractogram of samples: (a) nano-Al_2O_3 and (b) nano-Al_2O_3/kaolin (c) kaolin.

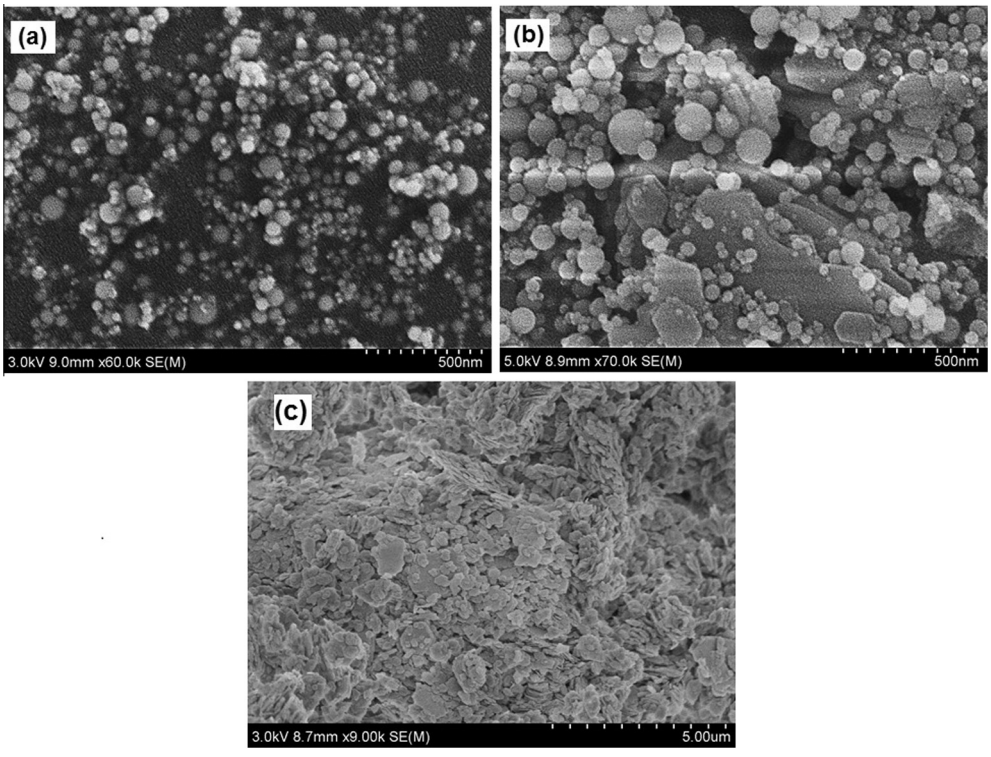

Figure 6 SEM images: (a) nano-Al_2O_3, (b) nano-Al_2O_3/kaolin and (c) kaolin.

Table 3 BET surface area analysis.

Sample	Kaolin	Nano-Al_2O_3	Nano-Al_2O_3/kaolin
BET surface area (m^2/g)	14.055	38.5	32.88

The Energy Dispersive X-ray (EDAX) spectra for composition analysis shown in Fig. 7(a–c) reveal that the silica content in pure kaolin gets reduced during the calcination process and the presence of trace silica in the composite was observed. Due to the conjunction of aluminium oxide nanopowder with kaolin, the purity of the aluminium oxide nanopowder had decreased to a minimal extent as seen in the EDAX spectra. To evaluate the effect of surface area of the photocatalysts, the BET surface area was measured and tabulated in Table 3.

3.2. Taguchi design and optimization of process parameters

The major process parameters influencing the spent wash decolourization were optimized using Taguchi orthogonal array design. The experimental design along with the observed responses is shown in Table 4. The results of the ANOVA test showed that the *p*-values of the model terms were significant, i.e. $p < 0.05$, for dosage which is the factor with major influence on decolourization (Table 5). The *p*-value indicates the significance of a particular term in a model. The *F*-values

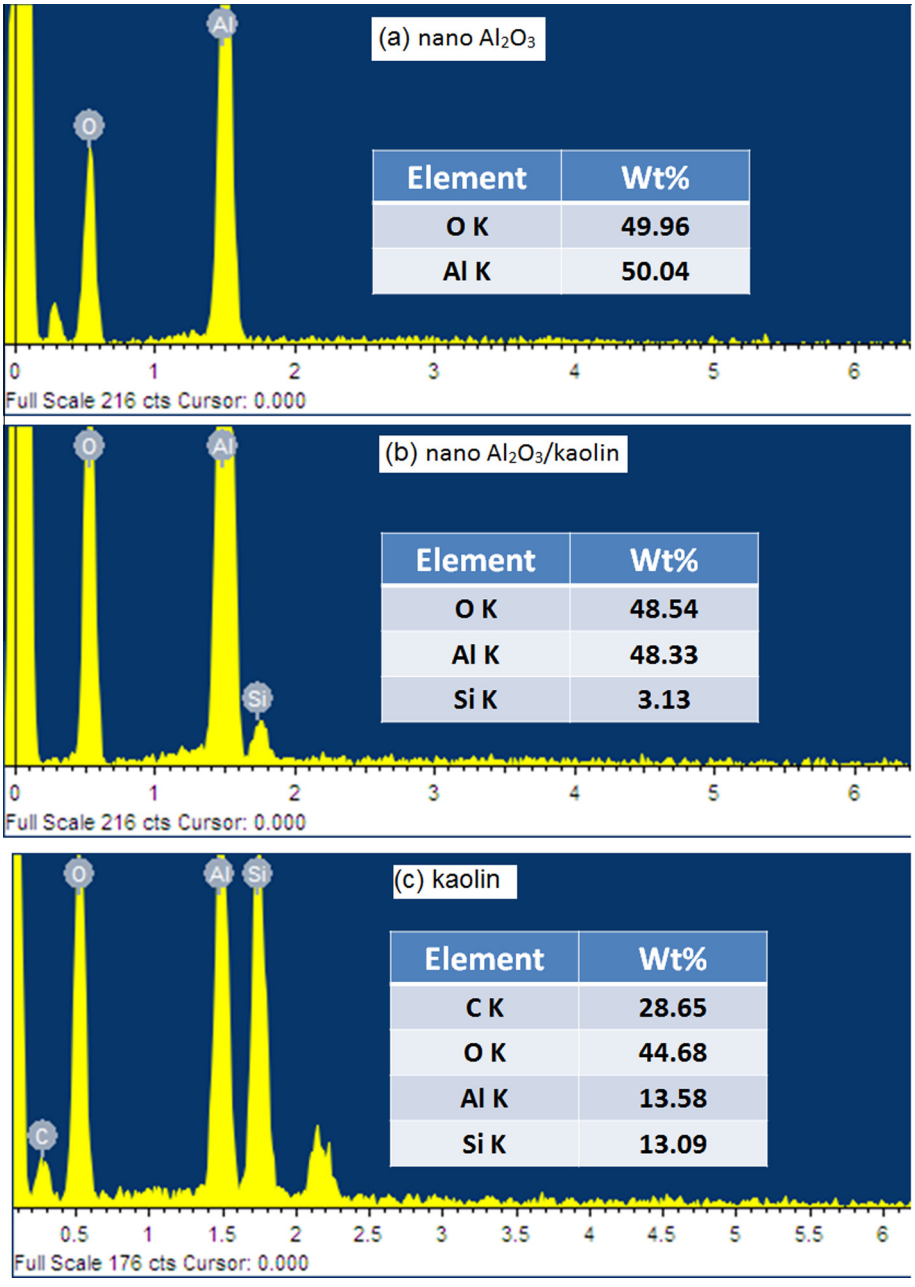

Figure 7 EDX spectrum and data of (a) nano-Al_2O_3, (b) nano-Al_2O_3/kaolin and (c) kaolin.

Table 4 Taguchi design with the process parameters along with experimental and predicted results.

Run No.	Catalyst dosage (*A*)	pH (g/l) (*B*)	Temp (°C) (*C*)	Agitation speed (rpm) (*D*)	Decolourization (%)		
					Experimental response	Predicted (Taguchi)	Predicted (ANN)
1	0.5	3	25	50	56.81	55.69	56.94
2	0.5	5	30	100	53.89	54.27	54.31
3	0.5	7	35	150	53.81	53.01	53.33
4	0.5	9	40	200	50.59	50.91	50.99
5	0.5	11	45	250	50.03	51.01	51.31
6	1.0	3	30	150	60.23	60.19	59.26
7	1.0	5	35	200	57.79	57.81	58.72
8	1.0	7	40	250	57.48	57.53	57.99
9	1.0	9	45	50	57.21	57.19	57.29
10	1.0	11	25	100	56.82	56.37	56.94
11	1.5	3	35	250	63.55	63.85	62.83
12	1.5	5	40	50	63.51	62.85	63.46
13	1.5	7	45	100	63.12	62.29	63.37
14	1.5	9	25	150	62.59	63.85	62.56
15	1.5	11	30	200	60.87	60.45	61.03
16	2.0	3	40	100	66.19	66.97	67.17
17	2.0	5	45	150	68.52	68.51	68.09
18	2.0	7	25	200	68.05	68.13	68.04
19	2.0	9	30	250	69.21	67.65	69.03
20	2.0	11	35	50	63.79	64.23	65.05
21	2.5	3	45	200	78.11	77.79	78.17
22	2.5	5	25	250	80.12	80.05	80.55
23	2.5	7	30	50	76.89	78.03	78.03
24	2.5	9	35	100	75.79	75.49	76.52
25	2.5	11	40	150	75.11	74.23	75.12

Table 5 ANOVA test for the response model for decolourization efficiency.

Source	DF	Seq SS	Adj SS	Adj MS	*F*	*P*
Dosage	4	31.1283	31.1283	7.7821	210.74	0.000
pH	4	0.8788	0.8788	0.2197	5.95	0.016
Temperature	4	0.3357	0.3357	0.0839	2.27	0.150
Agitation speed	4	0.0930	0.0930	0.0233	0.63	0.655
Error	8	0.2954	0.2954	0.0369		
Total	24	32.7312				

S = 0.192164, R-Sq = 99.10%, R-Sq(adj) = 97.29%

(Fisher test) showed the level of significance for the terms in the model, without defining the positive or a negative effect of that particular term. For catalyst dosage concentration, $F = 210.74$ which was greater than the *F*-values of the other process parameters.

3.3. Effect of process parameters on decolourization efficiency

The mutual interaction between the key process parameters in terms of spent wash decolourization was plotted. Surface plots showing interactions between catalyst dosage, pH *vs.* % decolourization, catalyst dosage, temperature *vs.* % decolourization and catalyst dosage, agitation speed *vs.* % decolourization are shown in Fig. 8. From the analysis of variance of the experimental data, it was clear that the catalyst dosage had a much impact in the decolourization efficiency followed by pH, temperature and agitation. With the highest value of $p = 0.655$, the agitation speed exhibited little impact on the process of decolourization of spent wash. For all the interactions involving catalyst dosage, % decolourization increased as the dosage concentration increased. The decolourization efficiency was found to be the highest at acidic conditions as shown in Fig. 8(a). At the lower temperature range of 25–30 °C, even minimal catalyst dosage concentrations resulted in better decolourization efficiency, whereas at higher catalyst dosage concentrations showed higher percentage colour removal irrespective of the operating temperature. There was not much of an influence by agitation speed on the decolourization efficiency. Optimization of the key process parameters *viz*. catalyst dosage, pH, temperature and agitation speed by Taguchi method led to 80% decolourization of the distillery spent wash effluent. A similar trend was also reported in the literature stating spent wash decolourization using optimized dosages of composite TiO_2 photocatalysts with 79% decolourization in the presence of solar light as an irradiation source [43] and MoO_3-TiO_2 nanocrystalline composite material for molasses decolourization under UV–visible radiation [44].

3.4. ANN analysis

A feedforward backpropagation model was developed with inputs of dimension-less variables such as catalyst dosage, pH, temperature and agitation speed. The output was in terms of decolourization efficiency. The input data were trained, validated and tested for best fit using the ANN tool. A two

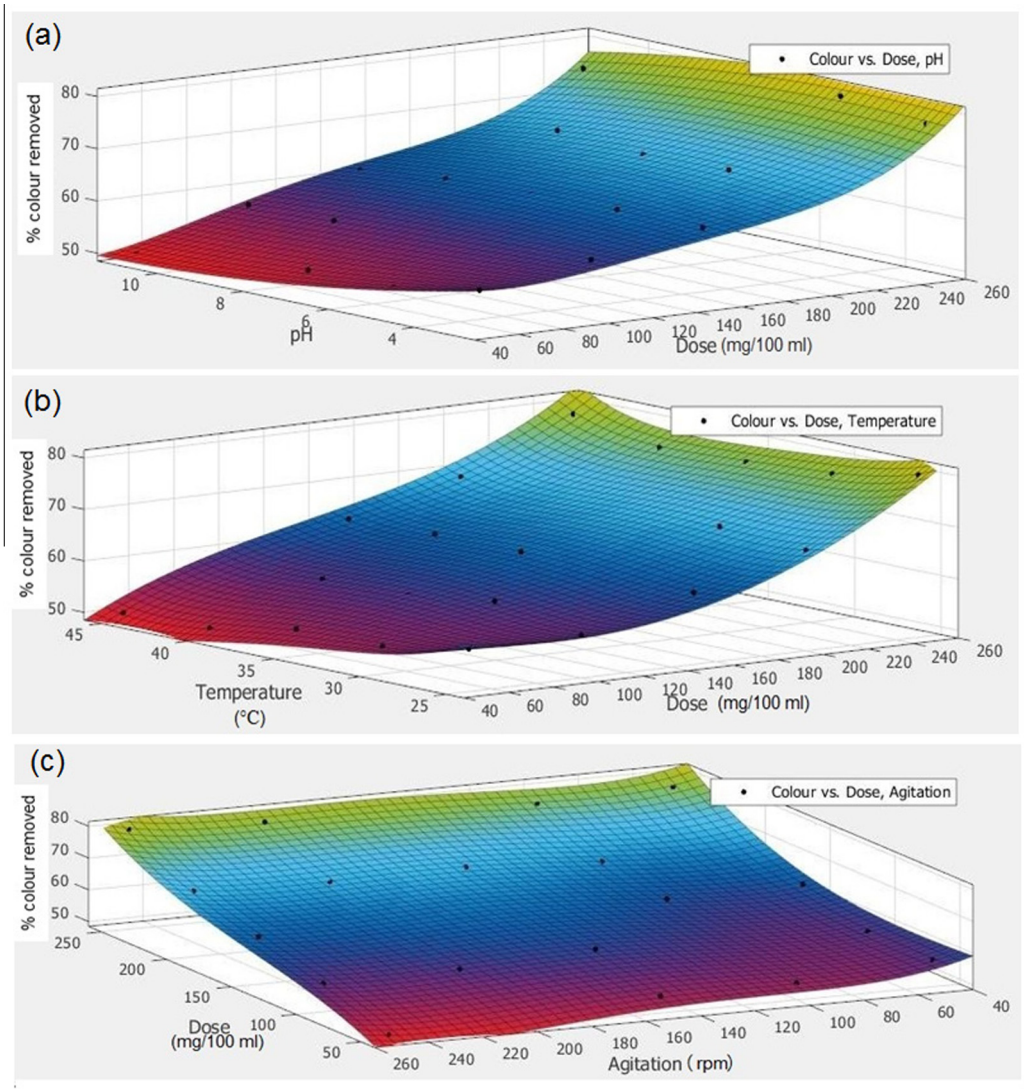

Figure 8 Surface plots showing interactions between catalyst dose, pH and temperature on percentage colour removal.

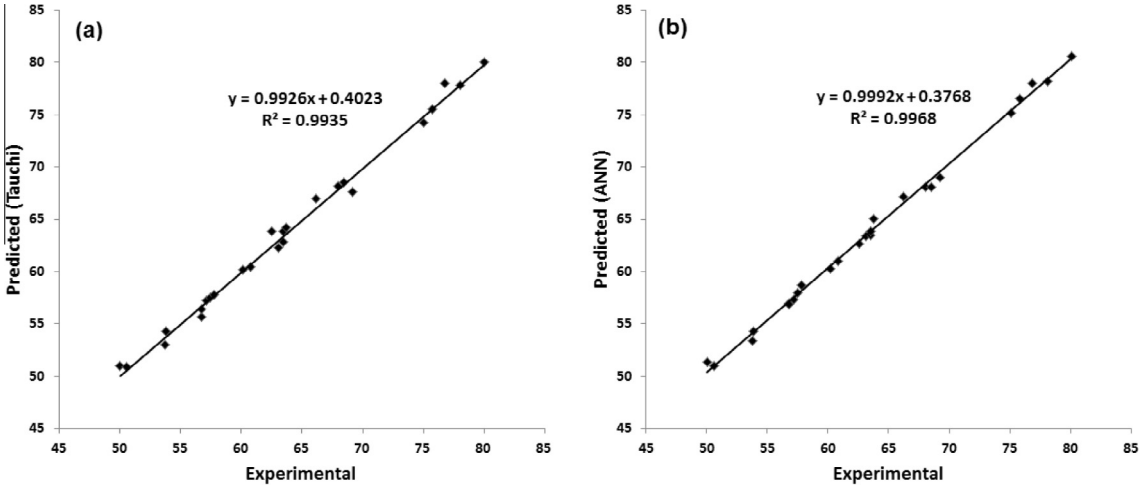

Figure 9 Experimental *vs.* predicted results for (a) Taguchi and (b) ANN.

layered network was used and the convergence took place at epoch 6 and at eighth iteration. The performance of the degradation process was evaluated using neural network and validated graphically. The gradient measure was 39.851, and correspondingly the *mu* reached minimum at epoch 3.

The weight factors and biases used in the ANN model are:

iw{1,1} wt to layer 1 from input 1:

[−0.14611 −1.3445 −1.1679 −0.076649;
1.871 0.50098 1.4415 −1.5989;
0.72351 −1.08 −0.66152 2.2127;
1.4004 0.63568 0.63846 −2.1889;
−1.8138 0.60207 2.0333 −0.91546;
−1.6675 2.1671 0.8139 −0.65725;
−0.22421 1.0256 0.040798 2.3339;
2.0841 −0.32986 1.5957 0.50367;
−1.7746 1.0018 1.3581 0.35448;
1.5241 −1.6066 0.88925 0.23574]

iw{2,1} wt to layer:

[0.50779 1.3218 0.47954 −0.51707 −0.36835
−0.47017 0.17978 −0.18025 0.0016846 −0.67646]

bias to layer 1:

[3.1995;
−1.4246;
−2.0042;
−0.37987;
0.19694;
−1.8613;
−0.40074;
1.7426;
−1.8782;
2.6989]

b{2} bias to layer 2:

[0.49917].

3.5. Analysis of predicted results of ANN and Taguchi

The result predicted by Taguchi and ANN was compared with the experimental results and plotted graphically (Fig. 9). The results predicted by ANN was found to be the best with an $R^2 = 0.9968$ compared to the $R^2 = 0.9935$ for Taguchi method.

4. Conclusion

The results indicated that the nano-Al_2O_3/kaolin composite photocatalyst prepared by calcination at high temperature, possessed and demonstrated good absorption of visible light range, which can degrade the intense colour of the distillery spent wash effluent. The key process parameters such as catalyst dosage, pH, temperature and agitation speed were optimized by Taguchi method and a maximum of 80% decolourization of distillery spent wash was achieved. The ANOVA studies of the mutually interacting key variables clearly revealed a strong correlation between the experimental and the predicted results. The optimized experimental input and the output data were fed as input data for the ANN tool to predict the error. A feedforward backpropagation method was used to predict the results. The efficacy of ANN and Taguchi for their ability to predict the spent wash decolourization efficiency was compared and ANN was found better in terms of predicting, data fitting and evaluation with an R^2 value of 0.9968. The study showed that the training of experimental data using ANN for decolourization of spent wash was found feasible. The ANN model prediction was found to be in good agreement with the experimental results.

Acknowledgments

Charles David is supported by the Technical Education Quality Improvement Program (TEQIP) Phase II, a World Bank initiative. The authors also thank the support of TEQIP-II and National Institute of Technology, Tiruchirappalli, Tamil Nadu, India, in this research work. The authors would like to extend their gratitude towards HRSEM facility (Funded by DST – India), Department of Chemical Engineering, IIT Madras, Chennai. Sincere thanks to Dr. Ramesh Babu and Mr. Arun Nellaiappan, Biomaterials Research Lab, Department of Metallurgy and Material Science, NIT Tiruchirappalli for XRD analysis.

References

[1] Y. Satyawali, M. Balakrishanan, Wastewater treatment in molasses based alcohol distilleries for COD and color removal: a review, J. Environ. Manage. 86 (2008) 481–497.
[2] V.P. Migo, M. Matsumara, E.J.D. Rosario, H. Kataoka, Decolorization of molasses wastewater using an inorganic flocculant, J. Ferment. Bioeng. 75 (1993) 438–442.
[3] N. Naik, K.S. Jagadeesh, M.N. Noolvi, Enhanced degradation of melanoidin and caramel in biomethanated distillery spent wash by micro-organisms isolated from mangroves, Iran. J. Energy Environ. 1 (2010) 347–351.
[4] P. Manisankar, C. Rani, S. Viswanathan, Effect of halides in the electrochemical treatment of distillery effluent, Chemosphere 57 (2004) 961–966.
[5] Y. Satyawali, M. Balakrishnan, Removal of color from biomethanated distillery spentwash by treatment with activated carbons, Bioresour. Technol. 98 (2007) 2629–2635.
[6] D. Pant, A. Adholeya, Biological approaches for treatment of distillery wastewater: a review, Bioresour. Technol. 98 (2007) 2321–2334.
[7] R.K. Prasad, Color removal from distillery spent wash through coagulation using *Moringa oleifera* seeds: use of optimum response surface methodology, J. Hazard. Mater. 165 (2009) 804–811.

[8] G.S. Kumar, S.K. Gupta, S. Gurdeep, Anaerobic hybrid reactor – a promising technology for the treatment of distillery spent wash, J. Ind. School Mines 11 (2007) 25–38.
[9] S. Venkatamohan, G. Mohanakrishna, S.V. Ramanaiah, P.N. Sarma, Simultaneous biohydrogen production and wastewater treatment in biofilm configured anaerobic periodic discontinuous batch reactor using distillery wastewater, Int. J. Hydrogen Energy 33 (2008) 550–558.
[10] S. Mohana, B.K. Acharya, D. Madamwar, Distillery spent wash: treatment technologies and potential applications, J. Hazard. Mater. 163 (2009) 12–25.
[11] H.H. Murray, Traditional and new applications for kaolin, smectite, and palygorskite: a general overview, Appl. Clay Sci. 17 (2000) 207–211.
[12] R.H. Zhao, F. Guo, Y.Q. Hu, H.Q. Zhao, Self-assembly synthesis of organized mesoporous alumina by precipitation method in aqueous solution, Microporous Mesoporous Mater. 93 (2006) 212–216.
[13] T.K. Sen, M.V. Sarali, Adsorption of cadmium metal ion (Cd^{2+}) from its aqueous solution by aluminium oxide and kaolin: a kinetic and equilibrium study, J. Environ. Res. Dev. 3 (2008) 220–227.
[14] J.C. Hughes, R.J. Gilkes, R.D. Hart, Intercalation of reference and soil kaolins in relation to physico-chemical and structural properties, Appl. Clay Sci. 45 (2009) 24–35.
[15] J.C. Miranda-Trevino, C.A. Coles, Kaolinite properties, structure and influence of metal retention on pH, Appl. Clay Sci. 23 (2003) 133–139.
[16] F. Bergaya, G. Lagaly, Handbook of Clay Science 2, second edition., Elsevier, 2013.
[17] D. Ghosh, K.G. Bhattacharyya, Adsorption of methylene blue on kaolinite, Appl. Clay Sci. 20 (2002) 295–300.
[18] R.G. Harris, J.D. Wells, B.B. Johnson, Selective adsorption of dyes and other organic molecules to kaolinite and oxide surfaces, Colloids Surf. A 180 (2001) 131–140.
[19] B.K. Nandi, A. Goswami, M.K. Purkait, Removal of cationic dyes from aqueous solutions by kaolin: kinetic and equilibrium studies, Appl. Clay Sci. 42 (2009) 583–590.
[20] L. Mingzhu, Y. Huaming, Large surface area mesoporous Al_2O_3 from kaolin: methodology and characterization, Appl. Clay Sci. 50 (2010) 554–559.
[21] N.J. Saikia, D.J. Bharali, P. Sengupta, D. Bordoloi, R.L. Goswamee, P.C. Saikia, P.C. Borthakur, Characterization, beneficiation and utilization of a kaolinite clay from Assam, India, Appl. Clay Sci. 24 (2003) 93–103.
[22] N. Salahudeen, A.S. Ahmed, A.H. Al-Muhtaseb, M. Dauda, S.M. Waziri, B.Y. Jibril, Synthesis of gamma alumina from Kankara kaolin using a novel technique, Appl. Clay Sci. 105 (2015) 170–177.
[23] M.M. Khan, S.A. Ansari, M.I. Amal, J. Lee, M.H. Cho, Highly visible light active Ag@TiO_2 nanocomposites synthesized using an electrochemically active biofilm: a novel biogenic approach, Nanoscale 5 (2013) 4427–4435.
[24] M.M. Khan, J. Lee, M.H. Cho, Au@TiO_2 nanocomposites for the catalytic degradation of methyl orange and methylene blue: an electron relay effect, J. Ind. Eng. Chem. 20 (2014) 1584–1590.
[25] M.M. Khan, S.A. Ansari, J.H. Lee, M.O. Ansari, J. Lee, M.H. Cho, Electrochemically active biofilm assisted synthesis of Ag@CeO_2 nanocomposites for antimicrobial activity, photocatalysis and photoelectrodes, J. Colloid Interface Sci. 431 (2014) 255–263.
[26] M.M. Khan, S.A. Ansari, M.O. Ansari, B.K. Min, J. Lee, M.H. Cho, Biogenic fabrication of Au@CeO_2 nanocomposite with enhanced visible light activity, J. Phys. Chem. C 118 (2014) 9477–9484.
[27] R. Saravanan, E. Thirumal, V.K. Gupta, V. Narayanan, A. Stephen, The photocatalytic activity of ZnO prepared by simple thermal decomposition method at various temperatures, J. Mol. Liq. 177 (2013) 394–401.
[28] R. Saravanan, V.K. Gupta, T. Prakash, V. Narayanan, A. Stephen, Synthesis, characterization and photocatalytic activity of novel Hg doped ZnO nanorods prepared by thermal decomposition method, J. Mol. Liq. 178 (2013) 88–93.
[29] R. Saravanan, H. Shankar, T. Prakash, V. Narayanan, A. Stephen, ZnO/CdO composite nanorods for photocatalytic degradation of methylene blue under visible light, Mater. Chem. Phys. 125 (2011) 277–280.
[30] R. Saravanan, S. Karthikeyan, V.K. Gupta, G. Sekaran, V. Narayanan, A. Stephen, Enhanced photocatalytic activity of ZnO/CuO nanocomposite for the degradation of textile dye on visible light illumination, Mater. Sci. Eng. C 33 (2013) 91–98.
[31] D.S. Nagesh, G.L. Datta, Prediction of weld bead geometry and penetration in shielded metal-arc welding using artificial neural networks, J. Mater. Process. Technol. 123 (2002) 303–312.
[32] Y.K. Mohanty, B.P. Mohanty, G.K. Roy, K.C. Biswal, Effect of secondary fluidizing medium on hydrodynamics of gas–solid fluidized bed—statistical and ANN approaches, Chem. Eng. J. 148 (2009) 41–49.
[33] J. Wang, W. Wan, Experimental design methods for fermentative hydrogen production: a review, Int. J. Hydrogen Energy 34 (2009) 235–244.
[34] P. Mullai, R.E. Rene, A simple multi layered neural network model for predicting bacterial xylanase production by *Bacillus* sp. using Avena sativa as substrate, Biotechnology 7 (2008) 499–508.
[35] J. Jasinski, M. Szota, L. Jeziorski, Neural networks application for modeling carbonizing process in fluidized bed, Int. Sci. J. 32 (2008) 103–108.
[36] A. Sahoo, G.K. Roy, Artificial Neural Network approach to segregation characteristics of binary homogeneous mixtures in promoted gas–solid fluidized beds, Powder Technol. 171 (2007) 54–62.
[37] J. Manickaraj, N. Balasubramanian, Estimation of the heat transfer coefficient in a liquid–solid fluidized bed using an artificial neural network, Adv. Powder Technol. (2008) 1–12.
[38] C. David, R. Narlawar, M. Arivazhagan, Performance evaluation of *Moringa oleifera* seed extract (MOSE) in conjunction with chemical coagulants for treating distillery spent wash, J. Indian Chem. Eng. 1 (2015) 1–12, http://dx.doi.org/10.1080/00194506.2015.1006147.
[39] C. Raghukumar, G. Rivonkar, Decolorization of molasses spent wash by the white rot fungus *Flavodon flavus*, isolated from marine habitat, Appl. Microbiol. Biotechnol. 55 (2001) 510–514.
[40] R.K. Prasad, S.N. Srivastava, Sorption of distillery spent wash onto fly ash: kinetics, mechanism, process design and factorial design, J. Hazard. Mater. 161 (2009) 1313–1322.
[41] S. Chandrasekhar, Influence of metakaolination temperature on the formation of zeolite 4A from kaolin, Clay Miner. 31 (1996) 253–261.
[42] K.H. Hu, Z. Liu, F. Huang, X.G. Hu, C.L. Han, Synthesis and photocatalytic properties of nano-MoS_2/kaolin composite, Chem. Eng. J. 162 (2010) 836–843.
[43] M.N. Vineetha, M. Matheswaran, K.N. Sheeba, Photocatalytic colour and COD removal in the distillery effluent by solar radiation, Solar Energy 91 (2013) 368–373.
[44] Madhukar Navgire, Ajeet Yelwande, Deepak Tayde, Balasaheb Arbad, Machhindra Lande, Photodegradation of molasses by a MoO_3-TiO_2 nanocrystalline composite material, Chin. J. Catal. 33 (2012) 261–266.